

# The Use of South African Spent Pulping Liquor to Synthesize Lignin Phenol-Formaldehyde Resins

Priyashnie Govender      B. M. Majeke  
Abiodun Oluseun Alawode      Johans F. Gorgens      Luvuyo Tyhoda

## Abstract

This study aims to investigate the potential of using lignin sourced from South African black liquor as a total phenol substitute in phenol-formaldehyde resins (PFRs), with a particular focus on bonding strength and curing properties. Four South African pulping-based lignins were used to synthesize these lignin-phenol formaldehyde resins (LPF100 resins), namely Eucalyptus Kraft lignin, Pine Kraft lignin, Bagasse Soda lignin, and Bagasse Steam Exploded lignin. Fourier-transform infrared spectroscopy, thermogravimetric analysis, and differential scanning calorimetry were used to determine structural and curing properties. These resins were then used directly (unmodified) as adhesives to test shear bonding strength ( $R_0$  LPF100 adhesives). To improve the bonding properties of the unmodified LPF100 adhesives, the LPF100 resins were modified via the addition of a crosslinker (hexamine) as well as a hardener (either glyoxal,  $R_1$ , or epichlorohydrin,  $R_2$ ). All  $R_0$  LPF100 adhesives fell below the GB/T 17657-2013 plywood standard of  $\geq 0.7$  MPa, with the Bagasse Soda LPF100 adhesive recording the highest bonding performance of 0.5 MPa, and the lowest curing temperature of 68°C. From the modified adhesives, the best performing were the Pine Kraft ( $R_1$ ) and the Eucalyptus Kraft ( $R_2$ ) LPF100 adhesives, recording 1.4 and 1.3 MPa, respectively. The curing temperatures of both these resins were 71°C and 80°C, respectively. Ultimately, the results of this study indicated that favorable adhesive properties may be obtained with the use of South African pulping-based lignins as a 100 percent phenol substitute in PFRs.

Phenol-formaldehyde resins (PFR) are commonly used as wood adhesives in wood construction and in the production of wood composites. This is because they exhibit excellent resistance properties and are known to produce high bonding strengths. However, there are problems associated with the use of PFR, the most significant of which is that phenol is derived from petrochemicals such as benzene and propylene. As a result, the cost of phenol is heavily influenced by the cost of crude oil, which itself is subject to dwindling reserves and price fluctuations (Alonso et al. 2005, Yang et al. 2014). These factors, coupled with growing environmental concerns over the impact of fossil fuels, have driven the need for a total or partial phenol replacement in phenol-based products.

Lignin, a biopolymer found in plant biomass, has great potential as a phenol substitute due to its phenolic structure, thermoplastic nature, and abundance as a byproduct of the paper and pulp industry, as well as the cellulosic ethanol industry. It also has high resistance to water and biodegradation, and is relatively cheaper and less toxic than phenol (Hu et al. 2011, Siddiqui 2013). However, despite its benefits and availability, lignin is rarely exploited for higher value applications. Instead, it is largely used as fuel for paper and pulp mills, and commercial applications

of lignin are mainly as surfactants, dispersants, and emulsifiers. This underutilization of lignin is largely attributed to its structural complexity and low reactivity, which is further aggravated by its structural diversity according to biomass origin, separation, and fragmentation processes. Thus, partial incorporation of lignin into a resin system usually results in decreased reactive functionalities within the polymeric structure. As a result, most research has found that lignin substitution up to 50 percent is capable of producing good bonding strengths, although other important resin properties such as curing and dimensional stability remain problematic. To address these issues, a

The authors are, respectively, Graduate Student and Graduate Student, Dept. of Process Engineering (Priyashnie.Govender@sappi.com, 16628233@sun.ac.za), Graduate Student, Dept. of Forest and Wood Sci. (aza0236@auburn.edu [corresponding author]), Professor, Dept. of Process Engineering (jgorgens@sun.ac.za), and Senior Lecturer, Dept. of Forest and Wood Sci. (ltyhoda@sun.ac.za), Stellenbosch Univ., South Africa. This paper was received for publication in September 2020. Article no. 20-00047.

©Forest Products Society 2020.  
Forest Prod. J. 70(4):503–511.  
doi:10.13073/FPJ-D-20-00047

number of modification methods have been developed to enhance lignin's chemical reactivity, as well as increase its solubility in organic solvents, improve its processability, and reduce its brittleness as lignin-based polymers. In contrast, few studies have successfully incorporated lignin into PFR at high substitution rates of 90 to 100 percent (Abdelwahab and Nassar 2011, Kalami et al. 2017). However, none of these methods have reached widespread commercialization thus far. Nonetheless, gradual progress in this field of research, ongoing environmental concerns, and the potential scarcity of petrochemicals has sustained the interest in developing economically feasible lignin valorization processes, particularly with regards to production of bio-based polymers (Effendi et al. 2008, Laurichesse and Avérous 2014, Yang et al. 2014).

Spent pulping liquor is a term used to describe the waste by-product stream that exits pulping processes. This spent pulping liquor consists largely of lignin and spent cooking chemicals, as well as other dissolved wood constituents. Spent pulping liquor is considered to be renewable and carbon neutral, so it is mostly burned as fuel to generate energy for the mills and recover cooking chemicals. However, conventional kraft pulping mills often experience difficulties at the recovery unit whereby excess spent pulping liquor, known as black liquor, causes a bottleneck at the recovery boilers, which ultimately limits pulp production (Siddiqui 2013, Namane 2016). A potential solution to this would be to divert the excess black liquor from the recovery unit, and potentially find a different but sustainable and viable use for it. Recent years have seen the South African paper and pulp industry become more interested in lignin derived from spent kraft pulping liquor, particularly as a phenol substitute in PFR and polyurethanes.

As a result, this study was commissioned to investigate the potential of using lignin derived from South African spent pulping liquor as a total phenol substitute (100%) in PFR. Lignins from various pulping processes (soda, kraft, and steam explosion), with various biomass origins (Eucalyptus, Pine, and Sugarcane Bagasse) were used, and the shear bonding strengths of the lignin-based resins were a focal point of the study.

## Materials

### Extraction of lignin from spent pulping liquor

The Pine Kraft (KF2-P-N), Eucalyptus Kraft (KF3-E-N), and Bagasse Soda (S-SCB-S) lignin samples were received in the form of spent pulping liquor. Lignin isolation was achieved by acid precipitation with 98 percent sulphuric acid ( $H_2SO_4$ ). Briefly,  $H_2SO_4$  was slowly added to the pulping liquor with gentle stirring until the pH dropped to 2 from an initial pH of approximately 12 to 13. Thereafter, the liquor was left to stand for a period of 24 hours, after which lignin was recovered by centrifugation at 7,000 revolutions per minute (rpm) for 10 minutes. The lignin was then washed twice with distilled water, air-dried overnight, and milled to a particle size of 0.5 mm. To ensure that the isolated kraft and soda lignins had minimal impurities, an acid purification step was employed. Briefly, the isolated lignin powders were suspended in a 1N sulphuric acid solution based on a proportion of 200 mL of acid solution for every 1 g of dried lignin. This suspension was allowed to mix for a period of 24 hours, after which the lignin was recovered by centrifugation at 7,000 rpm for 10 minutes.

The lignin solids were then washed twice with distilled water and air-dried overnight. The dried lignin powders were then milled to a particle size of 0.5 mm, and subsampled to ensure a uniform sample, after which they were stored in airtight plastic bags until further use. An overview of this process is given in Figure S1 of the supplementary material. The Bagasse Steam Exploded lignin (SE-SCB) was purchased from Sigma-Aldrich Pty. Ltd, South Africa. Preparation involved steam explosion of sugarcane bagasse, followed by alkali extraction of the lignin. The product was a dried purified powder; therefore, this sample required no further processing.

### Synthesis and development of resins, adhesives, and plywood boards

For the synthesis of the LPF100 resins, 37 percent formaldehyde and 98 percent NaOH was purchased from ScienceWorld. For the formulation of the lignin-based adhesives, glyoxal solution (40 weight% in  $H_2O$ ), analytical-grade epichlorohydrin ( $\geq 99\%$ ), and hexamine were purchased from Sigma-Aldrich Pty. Ltd. For the preparation of plywood samples, Douglas-fir veneers were supplied by a local wood mill, and Bondite 345, a commercial tannin-based wood resin, was supplied by Bondite (Pty) Ltd, South Africa.

## Methods

### Lignin characterization

Proximate analyses, such as moisture and ash content, were determined according to methods adapted from the National Renewable Energy Laboratory (NREL) standards NREL/TP-510-42621 (NREL 2008) and NREL/TP-510-42622 (NREL 2005), respectively. Elemental analysis of organic components in the oven-dried lignin samples were conducted at the Central Analytical Facilities of Stellenbosch University. A Vario EL Cube Elemental Analyser was used to determine the composition of carbon (C), hydrogen (H), nitrogen (N), and sulphur (S). Total sugar content was determined at the Sappi Technology Centre according to an in-house standard, using a Thermo Scientific High-Performance Anion Exchange Chromatography system equipped with Pulsed Amperometric Detection (HPAE-PAD).

Average weighted molecular weight ( $M_w$ ), number average molecular weight ( $M_n$ ), and the polydispersity ( $M_w/M_n$ ) of the lignin samples were determined by gel permeation chromatography (GPC). Prior to analysis, the bagasse and kraft lignins had to be acetylated according to Naron et al. (2017). Briefly, 0.5 g of each lignin sample was acetylated with 20 mL of a pyridine-acetic anhydride solution (50/50 volume%) at constant stirring for 24 hours at 25°C and 120 rpm. Thereafter, 100 mL of 0.1 M hydrochloric acid was added to mixture to precipitate the lignin and remove the pyridine. The lignin was recovered by centrifugation at 8,000 rpm for 5 minutes, after which it was washed twice with distilled water and air-dried. Approximately 4 mg of each acetylated sample was then dissolved in 2 mL of high-performance liquid chromatography (HPLC) -grade tetrahydrofuran (THF) stabilized with 0.125 percent butylated hydroxytoluene (BHT). The S-SCB-S sample dissolved in the solvent; therefore, it could not be analyzed any further because reprecipitation in the column would damage the column and interfere with the

analysis. The dissolved samples were then syringe-filtered into GPC vials prior to analysis. The GPC system consisted of a Waters 1515 isocratic HPLC pump, a Waters 717<sub>plus</sub> auto-sampler, a Waters 600E system controller (run by Breeze Version 3.30 SPA), a Waters in-line Degasser AF, a Waters 2414 differential refractometer used at 30°C, and a Waters 2487 dual-wavelength absorbance UV/Vis detector operating at variable wavelengths. THF stabilized with 0.125 percent BHT was used as the mobile phase at a flowrate of 1 mL/min. An injection volume of 100 µL was used, and the column oven was maintained at 30°C. Columns used included two PLgel (Agilent Technologies) 5 µm Mixed-C (300 by 7.5mm i.d.) columns and a precolumn, PLgel 5 µm Guard (50 by 7.5 i.d.). Calibration using narrow polystyrene standards ranging from 580 to 2 by 10<sup>6</sup> g/mol.

Fourier-transform infrared spectroscopy (FTIR) was performed using a Nicolet iS10 spectrometer (Thermo Scientific, Waltham, Massachusetts) equipped with a Smart iTR attenuated total reflectance (ATR) accessory, with a diamond crystal. Spectra were obtained in ATR mode at a resolution of 4 per cm, 64 scans per sample, and within the absorption bands in the 4,000 to 600 per cm region. Collection and processing of data was done with Thermo Scientific OMNIC software. Spectra was baselined-corrected, and assignment of absorption bands were based on relevant literature. To observe the thermal behavior of the lignin samples, thermogravimetric analysis (TGA) was performed using a TGA Q50 thermogravimetric apparatus. Approximately 5 ± 0.5 mg of sample was placed into an aluminum crucible, which was then loaded onto the TGA pan. Using a heating rate of 10°C/min, the analysis was conducted under argon atmosphere at 70 mL/min, from 20° to 30°C up to 595°C.

### Synthesis of LPF100 resins

The synthesis procedure was adapted primarily from Kalami et al. (2017), whilst synthesis parameter such as formalin/phenol (2.5) and NaOH/phenol (0.3) molar ratios were determined after consulting various relevant literature sources (Siddiqui 2013, Pfunzen 2015, Ghorbani et al. 2016, Kalami et al. 2017). Here, “phenol” refers to both lignin and phenol (as determined by the phenol substitution level), and molar ratios were based on the total amount of lignin/phenol used for each resin batch. In this study, 20 g of lignin was used as a basis for a resin batch; thus, the required amount of formalin was approximately 31.5 mL, and approximately 86 mL of 1M NaOH was used. The set-up for resin synthesis (Fig. 1) makes use of a round-bottom reaction flask fitted with a flat flange, a 5-port flange lid, flange clamp, heating mantle, a laboratory-scale overhead stirrer, a reflux condenser, dropping funnel, and a thermometer. Briefly, lignin was dissolved in two-thirds of the required 1M NaOH while stirring gently. Thereafter, formaldehyde was added to the reaction mixture, drop-wise, using the dropping funnel. The mixture was then allowed to stir for a few minutes, after which the mixture was gradually heated to 65°C whilst continuously stirring at 160 rpm. At 65°C, the reaction mixture was held at that temperature for 10 minutes, after which the last amount of NaOH was added drop-wise to the mixture. Thereafter, the reaction mixture was heated to a temperature of 85°C and held there for 1 hour. Finally, the heat was switched off and the mixture was left for 1 to 2 hours to cool to room

temperature. The liquid resins were then placed in Schott bottles and stored in the fridge at a temperature of ~13°C. For drying, the LPF100 resins were dried in a 40°C vacuum oven for approximately 24 hours. The oven was continuously purged with nitrogen to avoid build-up of any trace amounts of unreacted formaldehyde. Once dried, the resins were milled to a particle size of 0.5 mm, and then stored in airtight plastic bags until further use.

### Adhesive formulation

Initially, the LPF100 resins were used directly (unmodified) as adhesives (i.e., R<sub>0</sub> LPF100 adhesives). Alongside, an adhesive produced from a commercial wood resin, Bondite 345, was made. For each LPF100 resin, 8 g of resin was mixed with water at a water/resin mass ratio of 1. The commercial adhesive was prepared according to Alawode et al. (2019; i.e., 10 g of Bondite 345 and 2 g of hexamine were mixed together, after which the dry mixture was dissolved in 15 to 20 mL of distilled water).

To improve bonding strength performance, the LPF100 resins were modified by the addition of crosslinkers and hardeners, producing R<sub>1</sub> and R<sub>2</sub> LPF100 adhesives. Both R<sub>1</sub> and R<sub>2</sub> adhesives use the respective LPF100 resin together with hexamine as a crosslinker. The hardener glyoxal, which is biodegradable and nontoxic, was used for R<sub>1</sub> adhesives. The hardener epichlorohydrin, a highly effective agent used widely in industry, was used for R<sub>2</sub> adhesives. Using the amount of resin as a basis, the mass ratios of crosslinker/resin and hardener/resin were adapted from Alawode et al. (2019). Hexamine/resin was 0.2, glyoxal/resin was 0.45, epichlorohydrin/resin was 0.386, and water/resin was 1.87. Essentially, the dry powders were mixed together, after which the dry mixture was dissolved in water.

### Plywood preparation

Three-layer plywood boards were made using each of the different LPF100 adhesive samples. Specifications relating to the board, press conditions, and conditioning were adapted from literature (Imman et al. 2001, Alawode et al. 2019), as well as trial and error. Three-layered plywood samples of 9-mm thickness were prepared using 100 by 100 by 4-mm Douglas-fir veneers. The middle layer was coated with 350 g/m<sup>2</sup> of adhesive on either side, and then left exposed to air for 5 minutes to evaporate excessive moisture. The veneers were then arranged in such a way that the middle layer was perpendicular to the outer layers. The glued veneers were then hot-pressed for 10 minutes at 150°C. The boards were then left to cure in a conditioning room for 7 days, at a temperature of 20°C to 23°C and a relative humidity of 60 percent.

### Resin characterization

FTIR was performed to determine the chemical structure of the LPF100 resins. A Nicolet iS10 spectrometer (Thermo Scientific) equipped with a Smart iTR ATR accessory with a diamond crystal was used. Spectra were obtained in ATR mode at a resolution of 8 per cm, 32 scans per sample, and within the absorption bands in the 4,000 to 500 per cm region. Collection and processing of data were done with Thermo Scientific OMNIC software. Spectra were baselined-corrected, and assignment of absorption bands was based on relevant literature.

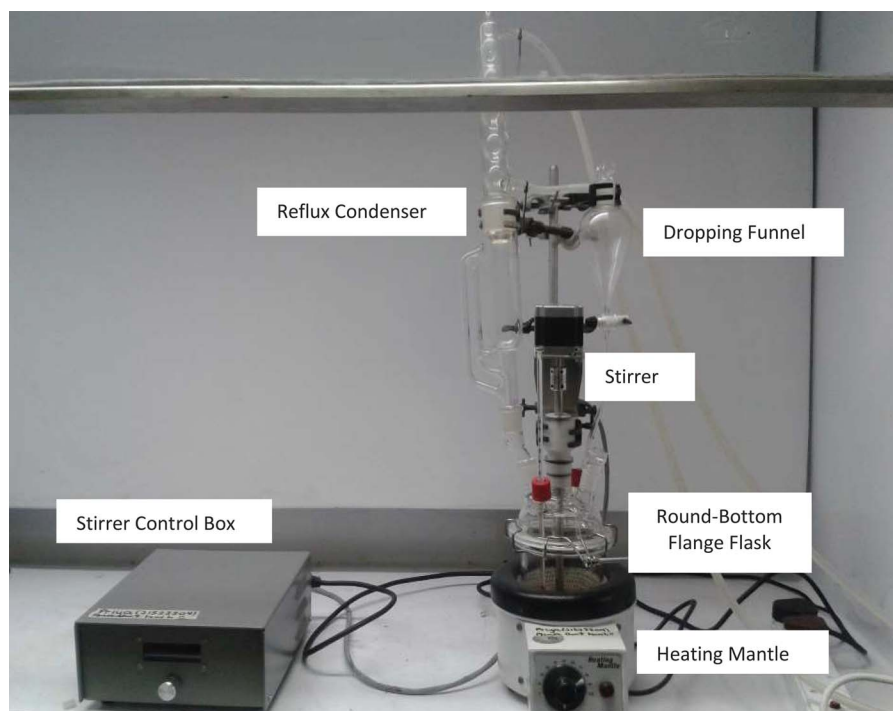


Figure 1.—Overview of experimental setup for resin synthesis.

To observe the thermal behavior of the LPF100 resin samples, TGA was performed using a TGA Q50 apparatus. Approximately  $5 \pm 0.5$  mg of sample was placed into an aluminum crucible, which was then loaded onto the TGA pan. Using a heating rate of  $10^\circ\text{C}$  per minute, the analysis was conducted from room temperature up to  $600^\circ\text{C}$ , under nitrogen atmosphere. The curing behavior of the LPF100 resins was observed by differential scanning calorimetry (DSC) using a TA Instrument Q100 calorimeter. Calibration of the instrument was done using an indium metal standard according to standard procedure. Approximately 4 mg of LPF100 resin was weighed into an aluminum pan and loaded onto the calorimeter; an empty aluminum pan was also loaded on as a reference. The samples were heated up at a rate of  $10^\circ\text{C}$  per minute over a temperature range of  $0^\circ\text{C}$  to  $250^\circ\text{C}$ , under nitrogen atmosphere.

Bonding strength was tested according to the ASTM International standard D906-98 (2011) for shear strength of plywood samples by tension loading. The plywood board specimens were cut according to the dimensions listed in the standard (25.4 by 82.5 mm). Three replicates of each board sample were obtained. Thereafter, the test specimens of each board sample were tested in a Zwick's Testing Machine. A test load was applied at a crosshead speed of 5 mm/min. Examples of the plywood samples are shown in Figure S2 of the supplementary material.

## Results and Discussion

### Lignin properties

Results from the proximate, elemental, and sugar analyses are summarized in Table 1. The ash content of the lignin samples is well below the recommended level of  $\leq 5$  percent for higher value applications. Additionally, they agree with literature in that the ash content of woody lignins are usually below 1 percent, whilst grasses generally possess

ash contents in the range of 2 to 5 percent. The total sugars content of the two kraft lignins and the SE-SCB lignin seems too minute to be quantified, whilst the S-SCB-S lignin has a negligible total sugars content of 0.25 percent. This could indicate that the soda process was not completely successful in breaking lignin-carbohydrate bonds. Ultimately, the sugar content of both the bagasse and kraft lignins is well below  $\leq 0.25$  weight percent. As such, it was concluded that this amount is not significant enough to interfere in any proceeding analyses, neither is it significant enough to negatively impact resin properties. Results from the elemental analysis of organic elements were consistent with ranges reported in literature (Mousavioun and Doherty 2010, Zhou et al. 2016, Naron et al. 2017, Kröhnke et al. 2019). All samples had negligible amounts of nitrogen ( $\leq 1\%$ ), which most likely originated from the biomass sources. The amount of elemental sulphur in the kraft samples were in the range of 3 to 9 percent, most of which would have originated from the isolation, precipitation, and/or purification processes that were employed. In contrast, the bagasse lignins had sulphur contents of  $< 1$  percent, which possibly originated from the biomass source, and, in the case of S-SCB-S lignin, the precipitation and purification steps.

The spectral results of the lignin samples are presented in Figure 2. The peak assignments of important functional bands are provided in Table S1 of the supplementary material. The broad peaks observed in the region of 3,440 to 3,430/cm are attributed to the stretching of aromatic and aliphatic hydroxyl (O-H) groups. Bands at 1,220 to 1,210/cm are typically assigned to the stretching of phenolic hydroxyl groups, specifically C-O stretching of phenolic C-OH and phenolic C-O (Ar) groups of guaiacyl (G) and syringyl (S) lignin monomeric units. The lignin samples showed distinctive peaks in this region, with the KF3-E-N lignin showing the lowest intensity, and the SE-SCB lignin

**Table 1.—Proximate, elemental (carbon [C], hydrogen [H], nitrogen [N], sulphur [S]), and sugar analysis (weight%, dry basis), molecular weights (g/mol), and polydispersity.<sup>a</sup>**

| Sample ID | Moisture content | Ash content | C    | H   | N   | S   | Total sugars | M <sub>w</sub> (g/mol) | M <sub>N</sub> (g/mol) | Polydispersity (M <sub>w</sub> /M <sub>N</sub> ) |
|-----------|------------------|-------------|------|-----|-----|-----|--------------|------------------------|------------------------|--|
| KF2-P-N   | 8.6              | 0.3         | 58.8 | 6.4 | 0.2 | 3.8 | 0.01         | 4,666                  | 1,848                  | 2.52   |
| KF3-E-N   | 7.5              | 0.4         | 58.1 | 5.9 | 0.2 | 4.0 | 0.00         | 3,071                  | 1,696                  | 1.81   |
| S-SCB-S   | 18.6             | 2.0         | 51.7 | 6.7 | 0.3 | 1.1 | 0.25         | NA                     | NA                     | NA   |
| SE-SCB    | 4.8              | 1.9         | 62.1 | 6.4 | 0.7 | 0.5 | 0.00         | 6,335                  | 2,263                  | 2.80   |

<sup>a</sup> M<sub>w</sub> = average weighted molecular weight; M<sub>N</sub> = number average molecular weight; NA = not available.

recording the highest intensity. This is a notable observation because phenolic hydroxyl groups in particular are the most reactive functional group and can significantly affect the reactivity of lignin. All lignins showed distinctive peaks in the region of 1,044 to 1,030/cm, assigned to stretching of primary aliphatic hydroxyls, specifically C–O stretching. Peaks at 2,849/cm, representing C–H vibration of methoxyl groups, were present in all samples, confirming the presence of methoxyl groups. Remaining bands are assigned to functional groups commonly found within the lignin structure. Bands at 2,935/cm are typical of C–H stretching, whilst bands at 1,712 to 1,702/cm are characteristic of conjugated ketones and aldehydes. The presence of peaks within 1,606 to 1,510/cm region are attributed to aromatic skeletal vibrations, and peaks within 1,426 to 1,424/cm indicates ring stretching coupled with C–H in-plane deformations. The bands within the region 914 to 813/cm are assigned to C–H bending of guaiacyl (G) and syringyl (S) units. Bagasse lignins also showed absorptions at 832/cm, which is characteristic of C–H stretching of H monomeric units.

The results obtained from GPC analysis are listed in Table 1. Looking at the kraft lignins, the KF2-P-N lignin possesses a higher weighted average molecular weight (M<sub>w</sub>, 4,666 g/mol) and polydispersity (2.52) than KF3-E-N lignin (3,071 g/mol and 1.81). This is consistent with results reported in literature. The SE-SCB lignin has a considerably higher M<sub>w</sub> (6,335 g/mol) and polydispersity (2.80) than

both kraft lignins, which is also in agreement with literature; Naron et al. (2017) characterized soda bagasse lignin and found the M<sub>w</sub> to be approximately 7,779 and the polydispersity to be 3.10.

The TGA curves of the lignin samples are given in Figure S3 of the supplementary material. The thermal decomposition profiles of the lignin samples, represented by the derivative thermogravimetric (DTG) curves, are presented in Figure 3. It is observed that the kraft and bagasse lignins experience their maximum degradation points within the temperature range of 350°C to 380°C, as reported in literature. It also seems that the KF2-P-N (Pine kraft) lignin is the most thermally stable because it experiences its maximum degradation rate at the highest temperature (~380°C). Once again, this could be due to the high guaiacyl composition of softwoods that have condensed C–C bonds, thereby making it very thermally stable.

## Resin and adhesive characterization

These spectral results are presented in Figure 4. The peak assignments of important functional bands are listed in Table S2 of the supplementary material. All resins exhibit a broad peak in the region of 3,400 to 3,200/cm, which is assigned to the stretching of OH groups. With particular interest to phenolic OH groups, all resins showed bands around 1,374/cm, which is characteristic of phenolic OH vibrations. Additionally, all resins exhibit weak peaks that appear at 1,458/cm, characteristic of C–H bending in CH<sub>2</sub>

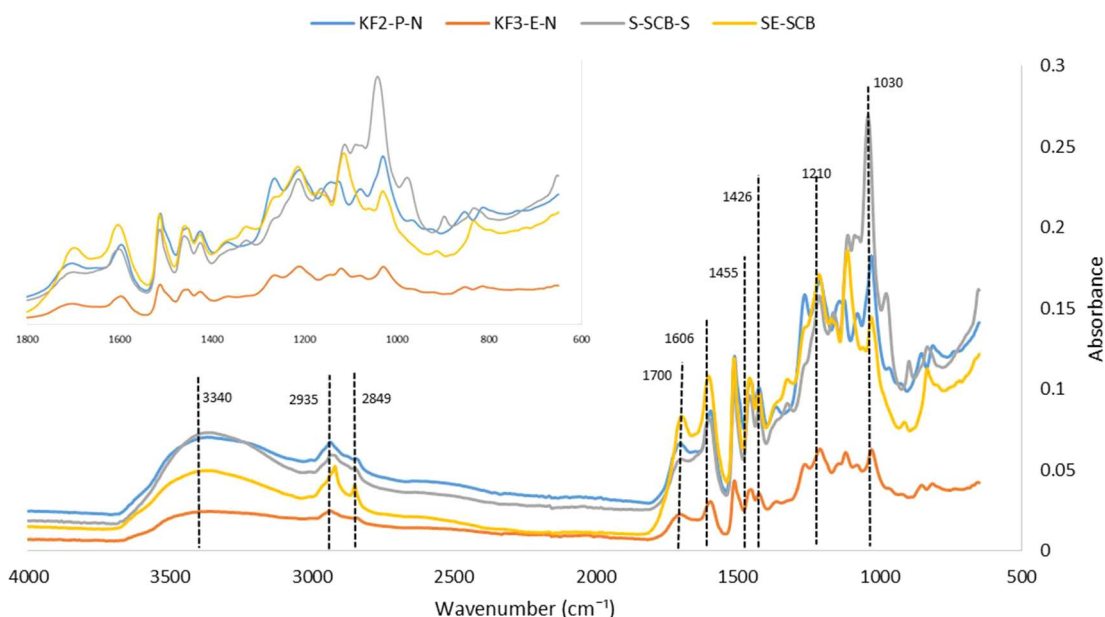


**Figure 2.—Fourier-transform infrared spectra of lignin samples.**



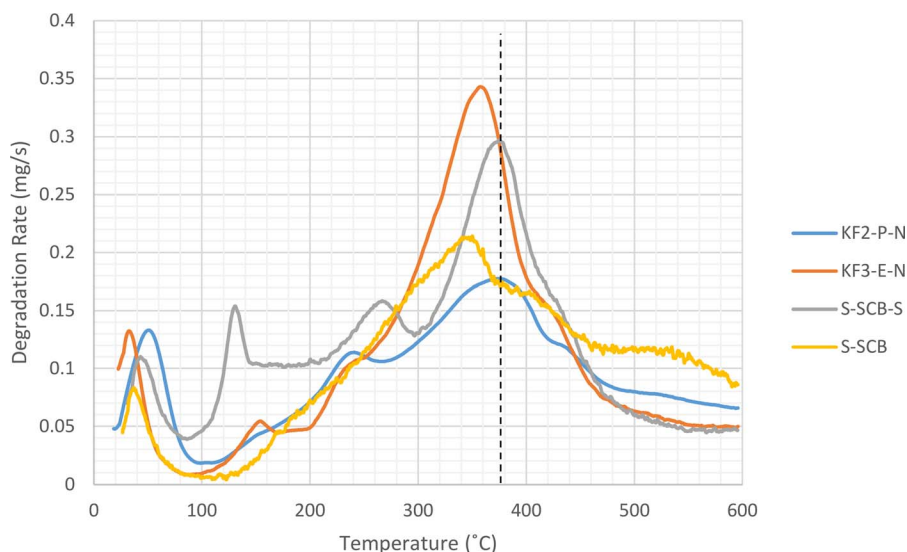


Figure 3.—Derivative thermogravimetric curve of lignin samples.

groups. This band is of particular interest because it indicates the presence of methylene bridges in the resin structure. During synthesis of PFRs, formaldehyde and phenol groups react to form methylolphenols, which then condense together, forming methylene or dimethylene ether bridges between them. Thus, the existence of these bridges gives a rough indication of the reaction between formaldehyde and the phenol moieties in lignin, as well as the condensation between the methylolphenols into some sort of prepolymer. This was further confirmed by the medium intensity absorption band at 1,020/cm in the kraft and SE-SCB resin spectra, which is characteristic of C–O stretching of methylol C–OH, aliphatic C–OH, and aliphatic C–O (Ar). Interestingly, all LPF100 resins showed very small peaks near the 2,724/cm band, which is an overtone band assigned to C–H bending in formaldehyde. This may indicate that

there were still small amounts of formaldehyde that did not take part in the resin synthesis reactions, possibly due to the well-documented limitations of the lignin molecule.

The TGA curves of the LPF100 resins are presented in Figure S4 of the supplementary material. It was found that all resins started to significantly degrade after 200°C, with the kraft resins and SE-SCB resin retaining 52 to 57 percent of their initial mass, and the S-SCB-S resin retaining about 42 percent of its initial mass. The weight residues of the resins at 595°C are given in Table S3 of the supplementary material, with the S-SCB-S and SE-SCB resins showing the lowest and highest thermal stability, respectively.

Differential scanning calorimetry (DSC) was then performed at a temperature range of 0°C to 200°C. The thermograms are displayed in Figure 5. A distinctive endotherm is observed for all resins, which is an indication

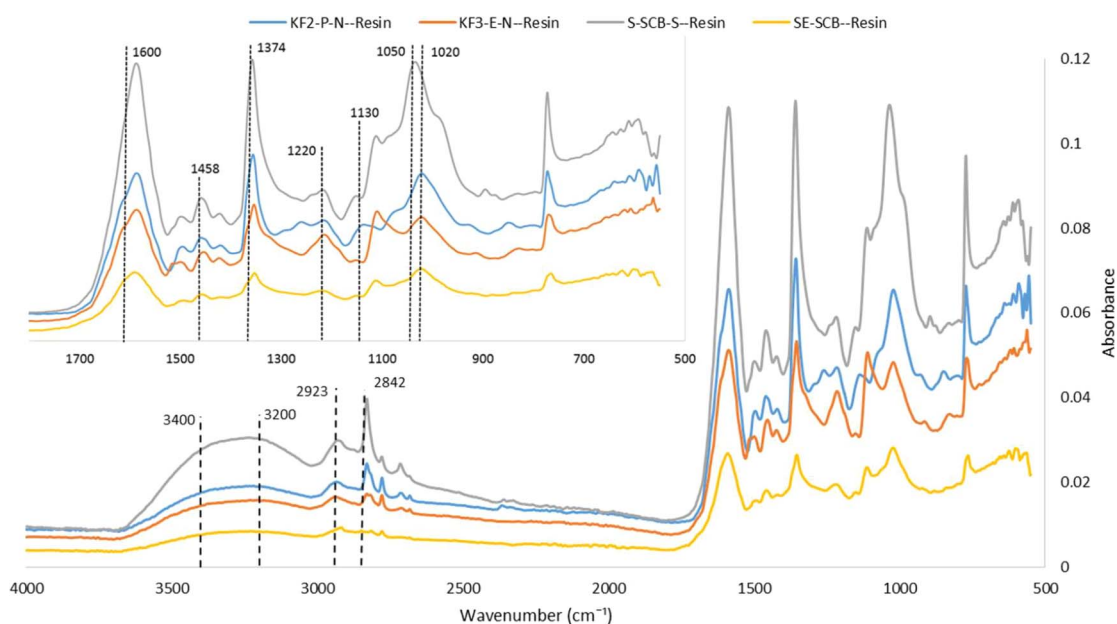


Figure 4.—Fourier-transform infrared spectra of LPF100 resin samples.

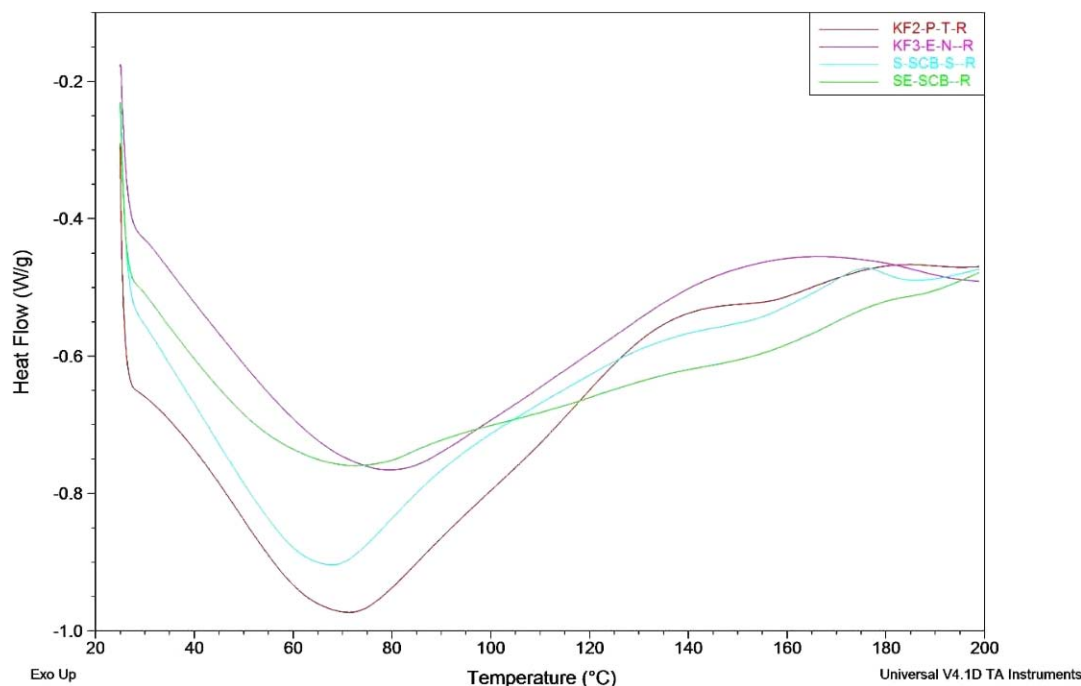


Figure 5.—Differential scanning calorimetry curves of LPF100 resins.

of resin curing. The onset temperatures ( $T_o$ ) of the resin samples, which marks the start of curing, are 27°C to 28°C. Peak temperatures ( $T_p$ ) of the resins are in the range of 70°C to 80°C. The difference of these two values,  $\Delta T$ , is the rate of curing, whereby a high  $\Delta T$  indicates a low rate of curing and vice versa. Correspondingly, the S-SCB-S resin has the highest cure rate with a  $\Delta T$  value of 40°C, and the KF3-E-N resin has the lowest cure rate at 52°C. The  $T_p$ ,  $T_o$ , and  $\Delta T$  values for the different resins are summarized in Table S4 of the supplementary material.

The performance of the  $R_0$  LPF100 adhesives was evaluated per the ASTM D906-98 (ASTM International 2011) standard. Results from these tests were assessed against the Chinese Grade A plywood standard (GB/T 17657-2013; Standardization Administration of China [SAC] 2013) whereby bonding strength should be  $\geq 0.7$  MPa for commercial use. These results are presented in Figure 6. The blue dotted line on Figure 5 represents the GB/T 17657-2013 standard. The maroon dotted line represents the shear bonding strength of the commercial tannin adhesive. Looking at the LPF100 adhesives ( $R_0$ ), none of them were able to meet the standard of  $\geq 0.7$  MPa. In contrast, the commercial tannin adhesive exceeded the standard, recording a shear bonding strength of 3 MPa. This performance of the commercial tannin adhesive is consistent with another study that used it as a reference adhesive, whereby the tannin adhesive produced a shear strength of 4.7 MPa.

Comparing the LPF100 adhesives ( $R_0$ ) with each other, it can be seen that the bagasse soda lignin (S-SCB-S) recorded the highest bonding strength of 0.5 MPa. The fact that these four LPF100 adhesives were able to effectively glue the wood veneers together and register a substantial bonding strength, speaks to their potential as wood glues.

However, given the below-standard performance of the LPF100 adhesives ( $R_0$ ), modification of the LPF100

adhesives ( $R_0$ ) was carried out to try to improve strength properties. This ‘modification’ would be carried out by addition of selected additives to the adhesive formulation to improve bonding performances, as described in the “Methods” section. The choice to modify the adhesive rather than the lignin sample was taken with the idea of practical industrial implementation in mind. If lignin as a feedstock is accompanied with the requirement of modification, of which no process to date has been able to successfully incorporate economic and environmental viability with efficient modification, it would significantly impede industrialization, as it does now. Thus, modification of the adhesive was chosen, especially because the addition of required additives are already industrially practiced. The shear bonding strength results of the LPF100 adhesives ( $R_1$  and  $R_2$ ) are also presented in Figure 6.

Looking at the LPF100 adhesives ( $R_1$ ), the best performing adhesive is the KF2-P-N adhesive with a shear bond strength of 1.4 MPa. This exceeds the GB/T 17657-2013 Chinese plywood standard (SAC 2013). Bagasse LPF100 adhesives showed no improvement in bonding strength, still registering shear strengths of 0.5 and 0.4 MPa for S-SCB-S and SE-SCB, respectively. Meanwhile, the KF3-E-N LPF100 adhesive ( $R_1$ ) could not undergo testing as the veneers of the board delaminated, qualitatively indicating poor bonding performance. Considering the LPF100 adhesives ( $R_2$ ), the overall bonding performances showed great improvement, with all LPF100 adhesives meeting or exceeding the standard of 0.7 MPa. The best performing adhesive was the KF3-E-N LPF100 adhesive ( $R_2$ ) with 1.2 MPa.

In general, it would seem that  $R_1$  adhesives using glyoxal did not enable improvement of bonding strength, with the exception of the KF2-P-N LPF100 adhesive ( $R_1$ ). On the other hand,  $R_2$  adhesives using epichlorohydrin

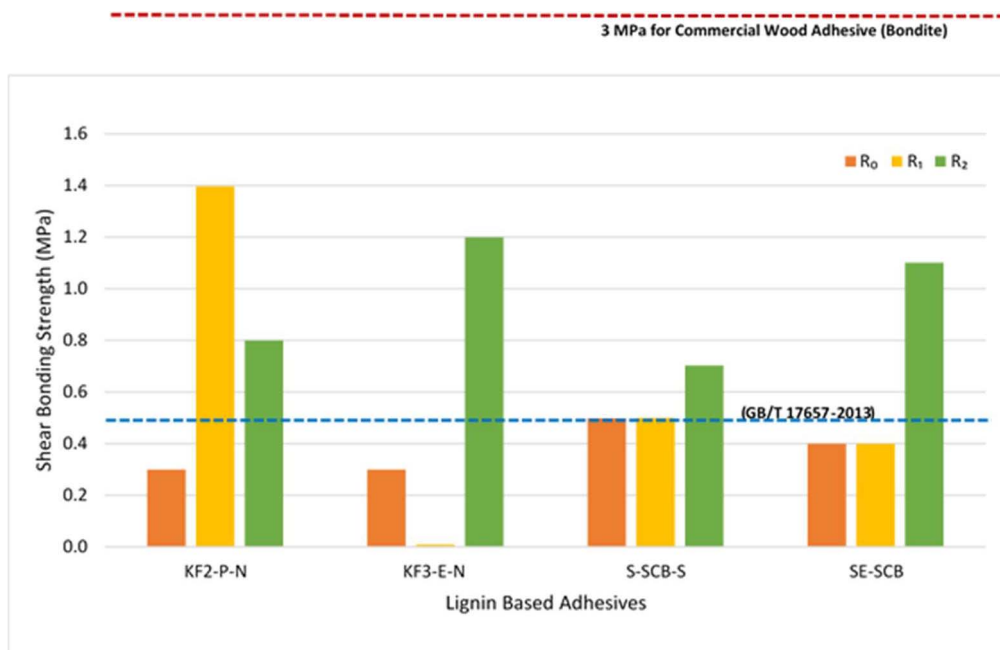


Figure 6.—Shear bonding strength of unmodified LPF100 adhesives ( $R_0$ ) and modified LPF100 adhesives ( $R_1$  and  $R_2$ ).

showed significant improvements, with all LPF100 adhesives ( $R_2$ ) meeting standard. To try to understand the variability in results across  $R_1$  and  $R_2$  test results, it is necessary to understand the reaction mechanism between the lignin-based resins, the wood, and the additives. Hexamine acts as a crosslinker via the trans-esterification reaction of its methoxyl groups with the hydroxyl groups present in the LPF100 resins, wood veneers, glyoxal ( $C_2H_2O_2$ ), and epichlorohydrin ( $C_3H_5ClO$ ). Its effectiveness as a crosslinker comes from the presence of six methoxyl methyl groups within its structure, thus providing a sufficient network of crosslinks by which hydroxyl groups in the LPF100 resin, wood, and hardeners can react with (Imman et al. 2001, Alawode 2019). The hexamine reacts with hydroxyl groups; therefore, the KF2-P-N and S-SCB-S adhesives would form a more extensive and stable crosslinked network with hexamine, due to the higher availability of phenolic hydroxyl groups. However, there is a difference in bonding strengths of  $R_1$  S-SCB-S and  $R_2$  S-SCB-S adhesives, which comes from the difference of hardener used. Similar results were reflected in the KF3-E-N and SE-SCB LPF100 adhesives, whereby improvements in bonding performance from  $R_0$  tests were only achieved in the  $R_2$  tests using epichlorohydrin. This could be attributed to the presence of ester groups within epichlorohydrin, which are more susceptible to reacting with the hexamine, because trans-esterification usually occurs between ester and alcohol groups. Meanwhile, glyoxal is a dialdehyde with carbonyl groups in its structure. In contrast, KF2-P-N LPF100 adhesives were the only adhesive to show improvements with the use of both  $R_1$  and  $R_2$  formulations, but with greater performance reflecting in  $R_1$  tests. Thus, there could be an interaction between glyoxal and a particular functional group within the KF2-P-N resin that allows for more effective cross-linking and curing.

## Conclusions

The objective of this study was to investigate the extent to which various South African pulping lignins were suitable for replacement of phenol in PFRs for use in the wood industry, specifically plywood boards. It was found that the synthesized LPF100 resins could not meet commercial plywood glue standards; however, the tested resin modification technologies proved to be a promising solution to this issue. In the end, the following conclusions can be drawn: From the LPF100 adhesives ( $R_0$ ), none were able to meet the standard of  $\geq 0.7$  MPa. They were also unable to match the performance of the commercial wood adhesive, Bondite (3 MPa). Looking at the modified LPF100 adhesives, the best performing were the KF2-P-N LPF100 adhesive ( $R_1$ ) and the KF3-E-N LPF100 adhesive ( $R_2$ ), recording 1.4 and 1.2 MPa of shear strength, respectively, thus exceeding the GB/T 17567-2013 plywood standard of  $\geq 0.7$  MPa (SAC 2013). However, considering that the KF3-E-N resin had the lowest curing rate, it is recommended the KF2-P-N (pine kraft) lignin be further investigated as a phenol replacement in PF resins. It should be noted the S-SCB-S resin was a consistent performer, recording 0.5 MPa for the  $R_0$  and  $R_1$  adhesives, and 0.7 MPa for the  $R_2$  adhesives. It also displayed the highest curing rate from all the resin samples. Thus, it also shows potential as a phenol substitute and is recommended for further investigation as a phenol substitute.

## Acknowledgments

The authors appreciate the Paper Manufacturers Association of South Africa (PAMSA) for financial support, and Sappi Limited (South Africa) for laboratory services.

## Literature Cited

Abdelwahab, N. and M. Nassar. 2011. Preparation, optimisation and characterisation of lignin phenol formaldehyde resin as wood adhesive. *Pigment Resin Technol.* 40(3):169–174.



- Alawode, A., P. Eselem-Bungu, S. Amiandamhen, M. Meincken, and L. Tyhoda. 2019. Properties and characteristics of novel formaldehyde-free wood adhesives prepared from *Irvingia gabonensis* and *Irvingia wombolu* seed kernel extracts. *Int. J. Adhes. Adhes.* 95:102423.
- Alawode, A. O. 2019. Properties and potential use of *Irvingia gabonensis* and *Irvingia wombolu* kernel extract as an eco-friendly wood adhesive. Doctoral thesis. Forestry and Wood Sciences Department, Stellenbosch University, South Africa.
- Alonso, M., M. Olié, F. Rodríguez, J. García, M. A. Gilarranz, and J. J. Rodríguez. 2005. Modification of ammonium lignosulfonate by phenolation for use in phenolic resins. *Biores. Technol.* 96:1013–1018.
- ASTM International. 2011. Standard test method for strength properties of adhesives in plywood type construction in shear by tension loading. ASTM D906-98. ASTM International, West Conshohocken, Pennsylvania.
- Effendi, A., H. Gerhauser, and A. Bridgwater. 2008. Production of renewable phenolic resins by thermochemical conversion of biomass: A review. *Renew. Sustain. Energy Rev.* 12:2092–2116.
- Ghorbani, M., F. Liebner, H. W. G. van Herwijnen, L. Pfungen, M. Krahofner, E. Budjav, and J. Konnerth. 2016. Lignin phenol formaldehyde resoles: The impact of lignin type on adhesive properties. *BioResources* 11(3):6727–6741.
- Hu, L., H. Pan, Y. Zhou, and M. Zhang. 2011. Methods to improve lignin's reactivity as a phenol substitute and as replacement for other phenolic compounds: A brief review. *BioResources* 6:3515–3525.
- Imman, S. H., S. H. Gordon, L. Mao, and L. Chen. 2001. Environmentally friendly wood adhesive from renewable plant polymer: Characteristics and optimization. *Polym. Degrad. Stabil.* 73:529–533.
- Kalami, S., M. Arefmanesh, E. Master, and M. Nejad. 2017. Replacing 100% of phenol in phenolic adhesive formulations with lignin. *J. Polym. Sci.* 134:45124.
- Kröhnke, J., N. Gierlinger, B. Prats-Mateu, C. Unterweger, P. Solt, A. Mahler, E. Schwaiger, F. Liebner, and W. Gindl-Altmutter. 2019. Comparison of four technical lignins as a resource for electrically conductive carbon particles. *BioResources* 14(1):1091–1109.
- Laurichesse, S. and L. Avérous. 2014. Chemical modification of lignins: Towards biobased polymers. *Prog. Polym. Sci.* 39:1266–1290.
- Mousavioun, P. and W. Doherty. 2010. Chemical and thermal properties of bagasse soda lignin. *Ind. Crops Prod.* 31(1):52–58.
- Namane, M. 2016. Precipitation and valorisation of lignin obtained from South African kraft mill black liquor. Doctoral thesis. University of KwaZulu-Natal, South Africa.
- Naron, D. R., F.-X. Collard, L. Tyhoda, and J. F. Gorgens. 2017. Characterisation of lignins from different sources by appropriate analytical methods: Introducing thermogravimetric analysis-thermal desorption–gas chromatography–mass spectroscopy. *Ind. Crops Prod.* 101:61–74.
- National Renewable Energy Laboratory (NREL). 2005. Determination of ash in biomass. NREL/TP-510-42622. NREL, Golden, Colorado.
- National Renewable Energy Laboratory (NREL). 2008. Determination of total solids in biomass and total dissolved solids in liquid process samples. NREL/TP-510-42621. NREL, Golden, Colorado.
- Pfungen, L. 2015. Lignin phenol formaldehyde wood adhesives. Master's thesis. University of Natural Resources and Life Sciences, Vienna.
- Siddiqui, H. 2013. Production of lignin-based phenolic resins using depolymerized kraft lignin and process optimization. Master's thesis. The University of Western Ontario, London, Canada.
- Standardization Administration of the People's Republic of China (SAC). 2013. Test methods of evaluating the properties of wood-based panels and surface decorated wood-based panels. GB/T 17657-2013. SAC, Beijing.
- Thies, M. C. and A. S. Klett. 2016. Recovery of low-ash and ultrapure lignins from alkaline liquor by-product streams. In: *Production of Biofuels and Chemicals from Lignin*, Biofuels and Biorefineries. Z. Fang, J. Richard, and L. Smith (Eds.). Springer Science+Business Media, Singapore. pp. 55–78.
- Yang, S., J.-L. Wen, T.-Q. Yuan, and R.-C. Sun. 2014. Characterization and phenolation of biorefinery technical lignins for lignin-phenol-formaldehyde resin adhesive synthesis. *R. Soc. Chem.* 4:57996–58004.
- Yang, S., Y. Zhang, T.-Q. Yuan, and R.-C. Sun. 2015. Lignin-phenol-formaldehyde resin adhesives prepared with biorefinery technical lignins. *J. Appl. Polym. Sci.* 132:42493.
- Zhou, H., D. Yang, and J. Y. Zhu. 2016. Molecular structure of sodium lignosulfonate from different sources and their properties as dispersant of TiO<sub>2</sub> slurry. *J. Dispers. Sci. Technol.* 37:296–303.